



HAL
open science

Uncovering the In Vivo Proxisome Using Proximity-Tagging Methods

Yoann G Santin

► **To cite this version:**

Yoann G Santin. Uncovering the In Vivo Proxisome Using Proximity-Tagging Methods. *BioEssays*, 2019, 10.1002/bies.201900131 . hal-02341404

HAL Id: hal-02341404

<https://amu.hal.science/hal-02341404>

Submitted on 31 Oct 2019

HAL is a multi-disciplinary open access archive for the deposit and dissemination of scientific research documents, whether they are published or not. The documents may come from teaching and research institutions in France or abroad, or from public or private research centers.

L'archive ouverte pluridisciplinaire **HAL**, est destinée au dépôt et à la diffusion de documents scientifiques de niveau recherche, publiés ou non, émanant des établissements d'enseignement et de recherche français ou étrangers, des laboratoires publics ou privés.

Uncovering the *in vivo* proxisome using proximity-tagging methods

Yoann G. Santin

Laboratoire d'Ingénierie des Systèmes Macromoléculaires, Institut de Microbiologie de la Méditerranée,
Aix-Marseille Université – CNRS UMR7255, 31 Chemin Joseph Aiguier, CS70071, 13402 Marseille
Cedex 09, France

Email: ysantin@imm.cnrs.fr

The ORCID identification number for the author: [0000-0003-1093-7465](https://orcid.org/0000-0003-1093-7465)

Twitter link: https://twitter.com/santin_yoann

Keywords: Protein-protein interaction, *in vivo* proximity labeling, APEX, BioID, PUP-IT,
proxisome, bacteria

33 **Summary**

34

35 The development of new approaches is critical to gain further insights into biological processes
36 that cannot be obtained by existing methods or technologies. The detection of protein-protein
37 interaction is often challenging, especially for weak and transient interactions or for membrane
38 proteins. Over the last decade, several proximity-tagging methodologies have been developed
39 to explore protein interactions in living cells. Among those, the most efficient are based on
40 protein partner modification, such as biotinylation or pupylation. Such technologies are based
41 on engineered variants of enzymes like peroxidases or ligases that release reactive molecules,
42 in the presence of specific substrates, that bind surrounding proteins. Fusing a protein of interest
43 to these enzymes allows the definition of an unbiased “proxisome”, that is all of the proteins in
44 interaction or in close vicinity of the protein of interest. Here, I describe the different proximity-
45 labeling tools available and provide a comprehensive comparison to discuss advantages and
46 limitations.

47

48

49

50

51

52

53

54

55

56

57 1. Introduction

58 By analogy with a theater play, biological processes require different actors assigned to perform
59 specific tasks in space and time. In living cells, such actors are mostly proteins that
60 “communicate” between each other. Communication is achieved through different types of
61 interactions such as weak, transient, stable or long interactions, resulting in specific biological
62 effects. Protein-protein interaction (PPI) can lead to conformational effects which enable the
63 formation of a structural complex, activate or inactivate a protein, create a new binding site for
64 the interaction with other binding partners or a substrate, serve as regulatory pathway, or allow
65 subcellular relocalization.

66 Detection of PPIs, in space and time, is therefore critical for deciphering each step of a
67 biological process. A number of methods for assaying PPIs *in vivo* have been developed and
68 are routinely used in laboratories. Co-immunoprecipitation (Co-IP) represents one of the most
69 standard methods of identifying interacting partners *in vivo*^[1,2]. Briefly, a protein of interest
70 (POI) is immunoprecipitated from a cellular protein extract by using specific antibodies
71 immobilized on beads (Fig. 1a). While unbound proteins are washed out, binding partners are
72 co-precipitated and can be visualized and identified by Western Blot or mass spectrometry
73 analysis. It is worthy to note that Co-IP is a variant of the pull-down assay, which used a tagged
74 bait protein to capture protein complexes instead of antibodies. Tandem affinity purification
75 (TAP) is also a systematic approach to detect PPIs at near proteome-scale under *in vivo*
76 conditions. TAP consists in two consecutive purifications by using two different tags fused to
77 a bait protein, then considerably reducing the amount of nonspecific contaminants^[3,4].
78 Additional methods such as two-hybrid systems, including bacterial (BACTH) and yeast (Y2H)
79 two-hybrid assays (see^[5] for comparative review), are powerful genetic approaches to
80 characterize PPIs in native or near-native context^[6-13]. POIs are fused to the two isolated
81 fragments from the *Bordetella pertussis* adenylate cyclase^[6,8-10,13] or from the Gal4

82 transcription factor^[7,11,12] for BACTH and Y2H respectively (Fig. 1b). Physical association
83 between tested proteins pairs restores the activity of the adenylate cyclase or Gal4 that can be
84 visualized by a transcriptional-activated reporter. Other interaction-mediated reconstitution-
85 based methods exist, such as the TOXCAT or GALLEX systems for studying transmembrane
86 helix-helix oligomerization in a natural membrane environment^[14-16]. With a similar conceptual
87 approach, Förster resonance energy transfer (FRET) is a well-suited biophysical method for the
88 investigation of PPIs that occur between two proteins positioned within 10 nanometers of each
89 other, allowing study of molecular interactions in real time^[17,18]. In brief, FRET relies on the
90 energy transfer from a donor fluorescent molecule (i.e., diminution of fluorescence intensity)
91 to an acceptor when these two probes are separated by 10 nanometers or less ^[19-22] (Fig. 1c).
92 Then, PPIs or conformational changes within a protein (if the two probes are fused to the same
93 protein) can be visualized in real time, by using a fluorometer or a fluorescence microscope.
94 Furthermore, this method can be extend to several practical applications in biology such as the
95 detection of protein cleavage, changes in micro-environment or quantitative analysis of protein
96 interactions (see^[23,24] for comprehensive reviews).

97 Although these methods have improved our knowledge about biological processes by the
98 characterization of number of PPIs, some important limitations are still present. Due to the
99 nature of stringent purifications, co-precipitation based-methods (i.e., Co-IP, pull down and
100 TAP) are not reliable to detect weak or transient PPIs, leading to a lot of false negatives^[25]. In
101 two-hybrid systems, proteins are produced from multi-copy plasmids and not at the
102 physiological concentration in the cell, which may cause unbalanced stoichiometry and effects
103 on PPIs, or toxicity within the cell^[26]. Proper re-assembly of the reporter is dependent of the
104 spatial association between the two tested proteins, hence steric effects may occur and prevent
105 detection of PPI. Screening only soluble domains of membrane proteins, which need the cell
106 membrane for proper folding, can lead to false negative in PPIs. Further, bait and prey proteins

107 are artificially put into the same subcellular compartment (i.e., the bacterial cytosol or the yeast
108 nucleus for BACTH and Y2H respectively), which may be different from the native
109 compartment of the POIs. Hence, protein pair could interact in a compartment where they
110 normally may not encounter each other or not interact if the physicochemical conditions are too
111 different from the native compartment(s). Finally, fluorescence based-methods suffer from
112 inherent physical and technical limitations. In FRET, since the distance between the donor and
113 the acceptor must be within the Förster radius (i.e., ~10 nm), poor positioning of fluorescent
114 probes in protein pair might lead to defect in detection of PPI. In addition, spectral leakage,
115 that correspond to the direct excitation of the acceptor and causing false positive detections,
116 donor fluorescence background, photobleaching and trouble for measurements make real PPI
117 detection quite difficult^[27].

118 Deciphering subtle PPIs in living cells is a challenge that cannot be achieved by those
119 conventional methods. Detection of weak and transient interactions, which constitute the major
120 part of PPIs in dynamic processes, interactions with membrane proteins and more importantly,
121 the detection in true *in vivo* context (i.e., both in native cell and at the chromosomal expression
122 level) must be improved to understand the complexity of biological processes. Over the last
123 decade, proximity-tagging approaches have been developed to explore these questions. Based
124 on protein partner modifications, proximity-tagging methodologies allow the definition of an
125 unbiased “proxisome”, that is all of the proteins in direct interaction or in close vicinity of the
126 POI, in native conditions and without loss of elusive PPIs. Currently, three major proximity-
127 tagging approaches are used: the proximity-dependent biotin identification (BioID), the APEX
128 proximity-dependent biotin labeling and the recent pupylation-based interaction tagging (PUP-
129 IT). Here, I detail the principles of these proximity-tagging methodologies and their different
130 applications in biology. Finally, I provide a comprehensive comparison to allow the definition
131 of the most appropriate approach for your studies.

132 2. Proximity-dependent biotin identification (BioID)

133 BioID is a useful proximity-dependent labeling method to screen both interacting and
134 neighboring proteins in their *in vivo* context. BioID assay is based on the promiscuous
135 biotinylation generated by a modified variant of BirA^[28,29]. BirA is a 35-kDa bacterial biotin
136 ligase that catalyzes the biotinylation of BCCP, a subunit of the acetyl-CoA carboxylase in
137 *Escherichia coli*^[30,31]. By using endogenous biotin and ATP, BirA produces biotinoyl-5'-AMP
138 molecules and biotinylates BCCP with an exquisite specificity. To perform proximity-
139 dependent labeling, the R118G mutant BirA protein (BirA^{R118G} or BioID protein) is used. This
140 variant, which normally binds ATP, displays a low affinity for biotinoyl-5'-AMP compared to
141 the WT BirA^[32]. Hence, biotinoyl-5'-AMP molecules are released from BioID protein and
142 covalently react with proximate proteins, and specifically on lysine residues, in a range of
143 approximately 10 nm^[33,34]. For BioID assay, promiscuous biotinylation is induced in cells
144 producing BioID fusion protein by adding a supraphysiological concentration of biotin in the
145 medium during an optimal labeling period of 16-18h^[34-36] (Fig. 2). Biotinylated proteins, which
146 are candidate interactors for the POI, are then enriched on streptavidin beads and identified by
147 mass spectrometry.

148 Recently, significant efforts have been made to improve BioID assay in living cells. Screen for
149 substitutions in the biotin binding site that modulate BirA activity revealed that R118K
150 substitution reduced biotin affinity and increased the biotinoyl-5'-AMP release^[37]. In 2016,
151 Kim and colleagues tested the potential of BirA protein from the thermophilic bacterium
152 *Aquifex aeolicus*^[38]. This variant, called BioID2, is 8-kDa smaller than BioID (i.e., 27 kDa) and
153 requires less biotin supplementation for proximity labeling^[38]. Interestingly, assaying for
154 dimerization-dependent protein interactions was investigated by split-BioID, where inactive
155 BioID-fragment complementation pair was generated as split-reporter and forms a functional
156 BioID protein that biotinylates substrates and other proximate proteins upon

157 heterodimerization^[39]. Finally, by using yeast display-based directed evolution, the Ting lab
158 recently engineered two enhanced BioID variants: the 35-kDa TurboID and the 28-kDa
159 miniTurbo^[40]. These variants display a remarkable labeling power, dropping from 16-18h to
160 only 10 min labeling period with similar size and specificity than standard BioID^[40].
161 Furthermore, proximity labeling activity of TurboID and miniTurbo is conserved in different
162 ranges of pH and at low temperature^[40] by contrast to BioID and BioID2 proteins^[38]. Taken
163 together, such improvements greatly extended the potentiality of the BioID system for assaying
164 proxisome detection in plethora of contexts.

165 BioID was initially developed for the study of the *in vivo* nuclear lamin-A proxisome in
166 mammalian cells^[34]. Up to now, BioID has been successfully used in diverse contexts. In
167 mammalian cells, BioID was applied to probe architecture of different subcellular locations
168 such as the nuclear pore complex^[33,41,42], focal adhesion complexes^[43] or the centrosome-cilium
169 interface^[44], and also to get insights about molecular mechanisms such as mitochondrial
170 proteostasis^[45,46], autophagy^[47], mitosis ^[48–50] or viral infection^[51]. BioID was also elegantly
171 adapted to investigate RNA-protein interactions that play important roles in cellular functions
172 and diseases. Named RaPID (for RNA–protein interaction detection), this method enables the
173 detection of proteins which interact with a specific RNA^[52]. Briefly, the RNA of interest is
174 flanked by bacteriophage BoxB stem loops which bind by the λ N peptide with high affinity^[53].
175 The λ N peptide is fused to the N-terminus of BioID protein. Then, BoxB stem loops recruit the
176 λ N-BioID fusion protein and thereby biotinylating proteins bound to the RNA of interest in
177 living cells^[52]. In addition, authors engineered BASU, a modified biotin ligase from *Bacillus*
178 *subtilis* that displays faster kinetics (>1000-fold) and increased signal-to-noise ratio (>30-fold)
179 compared to the standard *Escherichia coli* BioID protein. Although less active than miniTurbo
180 and TurboID^[40], BASU enabled sufficient labeling of proteins for RaPID study in living
181 cells^[52]. Finally, BioID was used for proximity labeling *in planta*^[54,55] and directly on animals

182 such as in mouse^[56] and recently in fruit flies (*Drosophila melanogaster*) and worms
183 (*Caenorhabditis elegans*)^[40].

184 **3. APEX proximity-dependent biotin labeling**

185 APEX is a spatially resolved proteomic mapping assay to determine *in vivo* proxisome in
186 dynamic systems in living cells. By contrast to BioID, APEX-dependent labeling is based on
187 the activity of the engineered enhanced hemic ascorbate peroxidase APEX, a 27-kDa
188 monomeric derivative of protein from soybean^[57,58]. Briefly, APEX catalyzes the H₂O₂-
189 dependent oxidation of phenol derivatives (the biotin-phenol, BP, being the most specific
190 substrate for APEX) into short lived phenoxyl radicals (<1 ms) that covalently react in a small
191 labeling radius (<20 nm) with electron-rich amino acids such as Tyr, Trp, His and Cys^[58]. It
192 has been recently established that tyrosine residues are the principal site of biotinylation by
193 APEX with more than 98 % labeling observed^[59]. Similar to BioID workflow, APEX labeling
194 starts with the construction of a functional fusion between APEX and the POI. After incubation
195 with BP, cells producing APEX fusion are treated with a 1-min pulse of hydrogen peroxide
196 enabling APEX-dependent biotinylation of proximate proteins in a short labeling radius (Fig
197 3)^[58,60]. Subsequently, cells are lysed and biotinylated proteins are purified and identified by
198 mass spectrometry analysis.

199 Due to its low activity when expressed at physiological level, APEX protein was further
200 improved to enhance its sensibility in living cells. By using directed evolution, a single point
201 substitution (A134P), located in a loop at the vicinity of both heme and the aromatic substrate-
202 binding site was found to confer great improvements in stability, kinetics, heme binding and
203 resistance to high H₂O₂ concentrations^[61]. Named APEX2, this variant is much more active
204 than APEX in the cell and is consequently better for proteomic mapping^[61]. Very recently, a
205 split-APEX (sAPEX) system has been developed^[62]. Two fragments called “AP” (a 200-amino-

206 acid N-terminal fragment) and “EX” (a 50-amino-acid C-terminal fragment) are each inactive
207 but give peroxidase activity upon reconstitution. Authors proposed that the sAPEX system
208 could be useful to address question about interaction-dependent proximity labeling at higher
209 spatiotemporal resolution. Hence, sAPEX reconstitution can be applied for mapping
210 specifically proxisome of target nucleic acids (e.g., mRNA, non-coding RNA or genomic locus)
211 by considerably reducing background caused by the activity of APEX2 that is not bound to the
212 target of interest^[63,64], or to capture molecular composition at the interface of two organellar
213 structures such as at mitochondria-ER contact^[62].

214 Over the past 6 years, many applications of APEX labeling have emerged to map proxisome
215 within specific locations and/or in dynamic molecular processes. Extensively used in eukaryotic
216 cells, APEX has been applied for investigating complex proteomes such as in human or in
217 *Drosophila melanogaster* mitochondria^[58,60,61,65–67], in mammalian cilia^[68] or in yeast Golgi^[69].
218 APEX proximity biotinylation was also used for exploring dynamic macromolecular complexes
219 within specific genomic loci or for RNA subcellular location. In order to define the human
220 mitochondrial nucleoid proteome, fusion between APEX2 and the mitochondrial DNA helicase
221 Twinkle was constructed and revealed new nucleoid-associated proteins^[70]. Last year, two
222 independent groups reported the development of GLoPro (for genomic locus proteomics) and
223 C-BERST (for dCas9 biotinylation at genomic elements by restricted spatial tagging), a
224 combination of CRISPR-based genome targeting with APEX2-dependent proximity labeling
225 for defining proteome at specific genomic locus^[63,64]. While receptor signaling constitutes a
226 critical process involved in numerous physiological regulations, tracking those processes
227 requires high spatio-temporal resolution and high throughput, missing in current methods.
228 Back-to-back papers from Kruse and Krogan labs elegantly demonstrated the application of
229 APEX assay to G-protein-coupled receptors signaling by tracking interactions at several
230 different time points upon addition of activating ligand and within a native cellular

231 environment^[71,72]. They finally concluded that APEX is a powerful method for spatially
232 resolved quantitative analysis of signaling, applicable to any other signal transduction
233 monitoring^[71,72]. Designed at the beginning for proteomic mapping, APEX has been recently
234 used for transcriptomic mapping assay. Spatial organization of RNA within the cell has been at
235 first determined by an indirect approach combining APEX proximity labeling with RNA-
236 protein chemical crosslinking^[73]. As this approach was inadequate for spatial specificity in
237 unenclosed cellular locations, authors introduced APEX-seq, a direct APEX-catalyzed labeling
238 of RNA combined with RNA-seq. This direct approach was successfully used in nine distinct
239 subcellular compartments allowing determination of a the RNA atlas in human cell^[74] and
240 recently the organization of translation initiation complexes^[75]. Finally, Zhou and colleagues
241 recently developed promising biotin-aniline and biotin-naphthylamine probes (Btn-An and Btn-
242 Nap, respectively), a new class of phenolic compounds with significantly higher reactivity
243 towards nucleic acids^[76]. Such developments open the field of new broad applications for *in*
244 *situ* transcriptomic assay to shed light on RNA functions in cell physiology.

245 Over the last year, APEX biotinylation assay was also performed in different microbial
246 pathogens such as for the mapping of the inclusion membrane proteins in *Chlamydia*
247 *trachomatis*^[77-80], in *Mycobacterium smegmatis* periplam^[81], in the diplomonad fish parasite
248 *Spiroucleus salmonicida*^[82], and in enteroaggregative *Escherichia coli* where stage-blocking
249 mutations were used to define *in vivo* temporal contacts of the TssA protein during type VI
250 secretion system biogenesis^[83]. With its broad range of applications in diverse organisms and
251 for labeling of different types of macromolecules, APEX proximity-dependent biotin labeling
252 constitutes a powerful tool for cellular processes that require high spatial specificity and short
253 labeling windows.

254 4. Pupylation-based interaction tagging (PUP-IT)

255 As a new proximity tagging method, the PUP-IT system was developed from the ubiquitin-like
256 process present in actinobacteria^[84–86]. The pupylation-based modification was extensively
257 studied in *Mycobacterium tuberculosis* for its implication in bacterial proteasome, a cellular
258 system required for causing disease^[85,87,88]. In this system, the Pup ligase PafA uses ATP to
259 transfer an activated Pup(E) substrate to a lysine of a target protein^[85,89,90]. Thereafter, the
260 Pup(E)-protein complex is targeted to the mycobacterial proteasome for unfolding and
261 degradation^[85,90,91]. Taking advantage of this system, Liu and colleagues adapted the Pup
262 system from *Corynebacterium glutamicum* as a PUP-IT tool to define membrane and
263 intercellular PPI^[92]. They first determined the potential of PafA to be a suitable proximity-
264 tagging enzyme and revealed that compared to BioID and APEX substrate, activated Pup(E)
265 does not freely diffuse from PafA, suggesting that very close proximity between the bait protein
266 and their partners is required for proper pupylation. They then tested *in vivo* PUP-IT by fusing
267 PafA to the membrane receptor CD28 to identify its cytosolic tail interactome (Fig. 4a). By
268 inducing the production of a biotinylated carboxylase-fused Pup(E) protein (bio-Pup(E)), which
269 was under the control of the locked TET-ON system^[93], the authors initiated the pupylation-
270 based labeling and successfully enriched known CD28-interacting proteins such as ITK, p85 or
271 LCK^[92]. They finally explored the possibility of extracellular PUP-IT labeling. To avoid long
272 exposure of PafA at the cell surface, authors induced the external heterodimerization of CD28
273 and PafA by using the FKBP-rapamycin-FRB system^[94] (Fig. 4b). Upon reconstitution, the
274 addition of ATP and truncated biotin-fused Pup(E) DE28 peptides (bio-DE28) enabled cell
275 surface labeling suggesting that PUP-IT can be used for extracellular pupylation^[92]. While the
276 PUP-IT has been only used in this study, it represents a promising method for assaying *in vivo*
277 PPIs especially involved in cell-to-cell communication, cell-to-cell adhesion, or host-pathogen
278 interactions.

279 **5. What is the best approach (for you)?**

280 Proximity-tagging methods can be used to circumvent inherent technical limitations that
281 conventional approaches for assaying *in vivo* PPIs suffer from. However, each of them display
282 differences which are both important or not depending on the nature of the study. In this section,
283 I will compare the specifications of each method to help defining the most suitable approach
284 for your studies.

285 **5.1. Advantages compared to conventional methods**

286 As mentioned in the introduction, proximity-tagging methods present many benefits compared
287 to conventional methods. First, interactome/proxisome of a POI can be defined under native
288 expression and stoichiometry by fusing tagging enzyme-coding gene at chromosomal locus of
289 the bait POI. Because proximate proteins are covalently labeled before purification, transient,
290 weak or hydrophobic interactions, which are lacking from some conventional methods, can be
291 easily detected. Further, promiscuous labeling of non-interacting-proximate proteins might be
292 useful to understand the environment of the POI and hence, to get new insights about its role
293 and/or its subcellular location in the cell. Interestingly, it has been shown that proxisome can
294 be expanded or reduced by modifying the length of the linker between the bait and the tagging
295 protein^[38]. As previously described, labeling molecules (i.e., biotinoyl-5'-AMP for BioID,
296 biotin-phenoxylys for APEX and Pup(E) for PUP-IT) have been shown not to cross plasma
297 membrane^[34,58,92], therefore proteome definition into cellular organelle or near to the membrane
298 might be useful to determine topology of transmembrane proteins^[58,67,95]. Finally, the use of
299 proximity-tagging methods in several biological contexts, ranging from the bacterial cell to the
300 living animals, makes them powerful versatile tools for investigating endogenous PPIs.

301 5.2. Common features to keep in mind before starting

302 As biological applications, proximity-tagging methods can be limited or be not suitable in
303 specific context.

304 First, characterization of the bait protein is a basic, but important prerequisite to confirm that
305 its location and its function in the cell are conserved in fusion with the tagging enzyme. Hence,
306 the use of proximity labeling method without preliminary results about the POI is strongly
307 discouraged.

308 While biotin is commonly used for detection and enrichment, it is necessary to examine
309 endogenous biotinylation occurring in your model organism. Overrepresentation of endogenous
310 biotinylated proteins might be detrimental by preventing enrichment of proximity labeled-
311 proteins, especially if the POI is thought to have only few partners. For example, in
312 *Mycobacterium smegmatis*, APEX2-dependent biotinylated proteins were confounded by
313 endogenous biotinylated proteins^[81]. To address this problem, authors successfully designed
314 two alternative labeling molecules: tyramide alkyne and tyramide azide, which can be used both
315 for detection and enrichment via a copper-catalyzed alkyne/azide cycloaddition “click”
316 reaction^[81]. Thus, the design of new probes could be a good option to circumvent this type of
317 issue in specific organisms.

318 Proximity labeling is associated with the presence and the accessibility of reactive residues such
319 as lysine in BioID^[28,34] and PUP-IT^[92] assay, and mostly tyrosine in APEX proximity-
320 labeling^[58,59]. Consequently, the efficiency of labeling is dictated by the composition and the
321 folding of proximate proteins. The absence of labeling does not therefore means a lack of
322 interacting or proximity partners, especially for proteins that lack of exposed Tyr/Lys. By
323 contrast, abundance of biotinylated proteins cannot be used to quantitatively assess the presence
324 or the strength of a putative interaction.

325 Except for PUP-IT system that requires contact for labeling^[92], labeling radius in BioID and
326 APEX assay is not a fixed value but instead a “cloud” or a “labeling gradient” where contours
327 depend on the physicochemical micro-conditions such as temperature or pH^[28,60]. By defining
328 a “proxisome”, it could be necessary to determine whether identified biotinylated proteins are
329 in direct interaction or in close proximity of the POI, especially if the POI is included within a
330 multiprotein complex.

331 Although weak, labeling of endogenous proteins present at many nanometers away from
332 tagging enzyme might be detected by MS analysis, especially in non-membrane-enclosed
333 cellular regions. Hence, efficient discrimination from proximate biotinylated proteins to the
334 cellular background is essential. To address this question, most studies combined proximity-
335 tagging methods with quantitative proteomics such as stable isotope labeling by amino acids in
336 cell culture^[43,60,63,66,95–97] (SILAC), tandem mass tagging^[64,70] (TMT), or label-free
337 quantification^[92] (LFQ). Schematic pipelines of these approaches applied to proximity-tagging
338 methods are represented in **Fig. 5**. Although there is no any report for preferentially using one
339 approach compared to another in the proximity-dependent labeling context, technical
340 specifications should be considered before starting your study. For example, SILAC and TMT
341 are much more expensive than LFQ but are more accurate for proteomic quantification.
342 Because LFQ is a non-ratiometric approach, there is no limit in multiplexing (i.e., the number
343 of conditions that can be tested simultaneously) by contrast to SILAC and TMT, limited to 5-
344 plex and 10-plex respectively. SILAC requires metabolically active cells to incorporate labels
345 whereas TMT can be directly performed on extracted peptides. Still, while LFQ presents a
346 better proteome coverage, it requires significantly longer data acquisition time compared to
347 SILAC or TMT. For the choice of the most suitable quantitative approach, see^[98] for recent
348 comprehensive comparison.

349 5.3. Comparative of the three approaches

350 To discriminate among those proximity-tagging methods, comparison of the main features
351 could be important for specific biological studies. In this context, I decided to distinguish
352 TurboID/miniTurbo assay (hereafter, (mini)TurboID assay) from BioID assay due to striking
353 differences in labeling process. All of the data are summarized in [Table 1](#).

354 APEX2, BioID2 and miniTurbo are relatively small proteins with a molecular mass of about
355 27 kDa^[38,40,58,61] while Turbo-ID, BioID and PafA proteins are larger, with a molecular mass
356 of about 35 kDa^[40], 35 kDa^[34] and 54 kDa^[92] respectively. Because the tagging-enzyme is fused
357 to the bait protein, its molecular mass can affect the localization and/or the function of the bait
358 protein in the cell. Thus, preliminary results about your POI can be useful to wisely determine
359 where you have to fuse the tagging-enzyme (i.e., in N or C-terminus of the POI), the nature of
360 the linker, in terms of residues and length, and the most suitable enzyme.

361 In BioID and (mini)TurboID assays, tagging-enzyme uses native ATP and exogenous input of
362 biotin as substrates for proximity labeling^[34,40]. Since biotin is essential for life, its
363 incorporation in cells is ensured by specialized transporters^[99]. By contrast, APEX2 uses H₂O₂
364 and non-natural phenol derivatives as substrates^[58,76,81]. Although in mammalian cells no
365 specific treatment is used for biotin-phenol incorporation, it has been reported that cell
366 permeability can limit biotin-phenol incorporation in yeast, preventing efficient labeling^[69]. In
367 *E. coli*, biotin-phenol uptake is in part mediated by the major γ -proteobacterium biotin
368 transporter YigM (Santin et al., unpublished data). Therefore, biotin-phenol incorporation
369 requires optimization for each organism. Finally, as non-natural compounds, whether phenol
370 derivatives affect cell growth needs to be examined for each case. During labeling, H₂O₂
371 treatment could affect the general cell oxidative state and cause cellular stress. Hence, APEX
372 assay is perhaps not suited for studies applied to oxidative stress or protein repair. In PUP-IT
373 assay, as Pup(E) derivative-peptides are not commercially available^[92], purification of these

374 substrates for extracellular labeling could be a limitation. However, Pup(E) substrates can be
375 genetically expressed in cells, and hence PUP-IT assay might be useful in organisms in which
376 substrate uptake is limiting.

377 To perform efficient *in vivo* labeling, the temperature in which the tagging-enzyme is active
378 has to fit with the growth temperature of the studied organism. In contrast to the BioID protein
379 that has an optimal temperature of 37°C^[34,38], BioID2 protein has optimal activity of 50°C,
380 yielding this enzyme well suitable for labeling in thermophilic conditions^[38]. Whereas BioID2
381 retains highly efficient biotinylation at 37°C, both BioID and BioID2 proteins exhibit reduced
382 activity below 37°C^[38]. APEX2, miniTurbo and TurboID proteins have an optimal activity at
383 37°C. Because these proteins were evolved from directed evolution in yeast (growing at 30°C),
384 they retain high activity at 30°C^[40,61]. In addition, miniTurbo and TurboID have been
385 successfully used in worms and flies which grow at 20°C and 25°C, respectively. While PafA
386 has only been tested in mammalian cells^[92] (37°C), the range of temperatures in which it retains
387 its activity has to be determined.

388 An important aspect of the proximity labeling is the temporal resolution of the reaction, both in
389 the control of the labeling initiation and in the labeling time. For example, definition of
390 signaling networks upon ligand-induced activation requires high temporal resolution^[71,72] in
391 contrast to studies about proteome definition in specific subcellular locations^[33,41,44,58,60,65,67].
392 In BioID and (mini)TurboID assays, the enzyme is active just upon translation and can use
393 endogenous biotin and ATP for proximity labeling, even before correct localization of the
394 fusion protein^[34,40]. In the PUP-IT assay, even though Pup(E) expression might be monitored,
395 invariable delay exists between induction and PafA mediated-pupylation^[92]. Hence, the
396 initiation of the labeling process may not be precisely controlled in these approaches. Finally,
397 as APEX-proximity labeling is nearly instant^[58,60,61], temporal control of the labeling can be
398 achieved by addition of H₂O₂ in the culture at specific time points. APEX assay is therefore

399 perfectly suited for taking snapshots of PPIs, for example in cellular response upon
400 environmental changes^[71,72] or during assembly of macromolecular complexes^[83]. With slow
401 tagging kinetics, the BioID and PUP-IT assays require 16-18 hours or 24-36 hours of labeling
402 time for efficient biotinylation/pupylation, respectively^[34,92]. These approaches are hence not
403 suited for capturing transient protein interactions but rather provide a history of protein
404 associations over long periods of time, as used in cell cycle^[48-50] or in viral infection^[51].
405 TurboID and miniTurbo were designed to improve BioID assay by reducing the labeling time
406 from 16-18 hours to 10 minutes^[40]. However, recent studies showed that this time might be
407 adapted depending on the organism studied. While 10 min are sufficient in mammalian cells^[40],
408 TurboID-mediated biotinylation requires about 30 minutes to 3 hours in yeast^[100], 4 hours in
409 flies^[40], 4 hours to several days in worms^[40] and 12 hours in plants^[101]. Optimization of the
410 TurboID labeling time should therefore be done for each organism, especially to prevent
411 toxicity via chronic endogenous biotinylation or endogenous biotin consumption due to the
412 high activity of these enzymes^[40].

413 Finally, BioID and (mini)TurboID assays have never been tested for extracellular labeling by
414 contrast to APEX^[102] and PUP-IT^[92]. Nevertheless, as PUP-IT and BioID-derivative assays use
415 a similar combination of ATP and substrates (Pup(E) and biotin, respectively), there is no
416 reason why BioID and (mini)TurboID should not work for extracellular labeling.

417 **6. Conclusions and prospects**

418 In molecular biology, the major question is: who acts in that process? To address this question,
419 many PPI-assaying methodologies have been designed for decades. However, technical
420 limitations in detection of PPIs in living cells, such as weak, transient or hydrophobic
421 interactions, prevent global comprehension. By providing both *in vivo* spatiotemporal
422 information and high-throughput analysis, proximity-tagging methods represent the next

423 generation of *in vivo* PPIs assay. In addition to the major proximity-tagging methods presented
424 in this review, other technologies exist including for example horseradish peroxidase-
425 dependent labeling approaches (EMARS^[103,104] and SPPLAT^[105–107]), photoactivated *in vivo*
426 proximity labeling^[108], NEDDylator system^[109,110] and methylation-based chromatin profiling
427 approach DamID^[111,112]. While proximity-tagging methods have been used in a variety of
428 biological contexts, further challenges remain to be overcome. For example, in thermophilic
429 organisms, such as archaea, where tools available for PPIs assay are limited^[113], or in protein-
430 lipid interactions, involved in many diseases including cancer, obesity, neurodegenerative
431 disorders or cardiovascular pathologies^[114]. However, over the last decade, the rapid
432 development of these proximity-tagging methods, in specificity and spatio-temporal control,
433 has revealed their potential to answer deeply questions in molecular biology. One may assume
434 that other applications will be made in the near future to further unravel the molecular
435 complexity in living cells.

436 **Abbreviations**

437 PPI, protein-protein interaction; POI, protein of interest; Co-IP, Co-Immunoprecipitation; TAP,
438 Tandem Affinity Purification; BACTH, bacterial adenylate cyclase-based two-hybrid; Y2H,
439 yeast two-hybrid assay; FRET, Förster resonance energy transfer; APEX, APEX proximity-
440 dependent biotin labeling BioID, proximity-dependent biotin identification; PUP-IT,
441 pupylation-based interaction tagging; SILAC, stable isotope labeling by amino acids in cell
442 culture; TMT, tandem mass tagging; LFQ, label-free quantitation.

443 **Acknowledgments**

444 I would like to thank Eric Cascales for support, Dukas Jurėnas for language editing, Etienne
445 Vanlioglu for discussions on mass spectrometry analysis, Camille Laberthonnière for helpful
446 advices, the members of the Cascales research group for useful discussions, and Yamamoto
447 Kadėrapė for encouragements. Research in Cascales laboratory is supported by the Centre
448 National de la Recherche Scientifique, the Aix-Marseille Universitė, and grants from the

449 Agence Nationale de la Recherche (ANR-14-CE14-0006-02, ANR-17-CE11-0039-01), the
450 Fondation pour la Recherche Médicale (DEQ20180339165), and the Fondation Bettencourt-
451 Schueller. My PhD work is supported by a doctoral fellowship from the French ministry of
452 higher education and research. All the figures were created with BioRender.

453 **References**

- 454 [1] J.-S. Lin, E.-M. Lai, *Methods Mol. Biol. Clifton NJ* **2017**, 1615, 211.
- 455 [2] C. Lee, *Methods Mol. Biol. Clifton NJ* **2007**, 362, 401.
- 456 [3] O. Puig, F. Caspary, G. Rigaut, B. Rutz, E. Bouveret, E. Bragado-Nilsson, M. Wilm,
457 B. Séraphin, *Methods San Diego Calif* **2001**, 24, 218.
- 458 [4] G. Rigaut, A. Shevchenko, B. Rutz, M. Wilm, M. Mann, B. Séraphin, *Nat. Biotechnol.*
459 **1999**, 17, 1030.
- 460 [5] J. Mehla, J. H. Caufield, N. Sakhawalkar, P. Uetz, *Methods Enzymol.* **2017**, 586, 333.
- 461 [6] A. Battesti, E. Bouveret, *Methods San Diego Calif* **2012**, 58, 325.
- 462 [7] S. Fields, O. Song, *Nature* **1989**, 340, 245.
- 463 [8] G. Karimova, J. Pidoux, A. Ullmann, D. Ladant, *Proc. Natl. Acad. Sci. U. S. A.* **1998**,
464 95, 5752.
- 465 [9] G. Karimova, N. Dautin, D. Ladant, *J. Bacteriol.* **2005**, 187, 2233.
- 466 [10] G. Karimova, E. Gaudiard, M. Davi, S. P. Ouellette, D. Ladant, *Methods Mol. Biol.*
467 *Clifton NJ* **2017**, 1615, 159.
- 468 [11] J.-S. Lin, E.-M. Lai, *Methods Mol. Biol. Clifton NJ* **2017**, 1615, 177.
- 469 [12] J. Mehla, J. H. Caufield, P. Uetz, *Cold Spring Harb. Protoc.* **2015**, 2015, 425.
- 470 [13] S. P. Ouellette, G. Karimova, M. Davi, D. Ladant, *Curr. Protoc. Mol. Biol.* **2017**, 118,
471 20.12.1.
- 472 [14] F. Hennecke, A. Müller, R. Meister, A. Strelow, S. Behrens, *Protein Eng. Des. Sel.*
473 *PEDS* **2005**, 18, 477.
- 474 [15] W. P. Russ, D. M. Engelman, *Proc. Natl. Acad. Sci. U. S. A.* **1999**, 96, 863.
- 475 [16] D. Schneider, D. M. Engelman, *J. Biol. Chem.* **2003**, 278, 3105.
- 476 [17] F. Festy, S. M. Ameer-Beg, T. Ng, K. Suhling, *Mol. Biosyst.* **2007**, 3, 381.
- 477 [18] R. Roy, S. Hohng, T. Ha, *Nat. Methods* **2008**, 5, 507.
- 478 [19] H. J. Carlson, R. E. Campbell, *Curr. Opin. Biotechnol.* **2009**, 20, 19.
- 479 [20] L. He, T. D. Bradrick, T. S. Karpova, X. Wu, M. H. Fox, R. Fischer, J. G. McNally, J.
480 R. Knutson, A. C. Grammer, P. E. Lipsky, *Cytom. Part J. Int. Soc. Anal. Cytol.* **2003**, 53, 39.

- 481 [21] I. T. Li, E. Pham, K. Truong, *Biotechnol. Lett.* **2006**, *28*, 1971.
- 482 [22] B. A. Pollok, R. Heim, *Trends Cell Biol.* **1999**, *9*, 57.
- 483 [23] B. Hochreiter, A. P. Garcia, J. A. Schmid, *Sensors* **2015**, *15*, 26281.
- 484 [24] K. Okamoto, Y. Sako, *Curr. Opin. Struct. Biol.* **2017**, *46*, 16.
- 485 [25] T. Branon, S. Han, A. Ting, *Biochemistry* **2017**, DOI 10.1021/acs.biochem.7b00466.
- 486 [26] A. Brückner, C. Polge, N. Lentze, D. Auerbach, U. Schlattner, *Int. J. Mol. Sci.* **2009**,
487 *10*, 2763.
- 488 [27] S. J. Leavesley, T. C. Rich, *Cytom. Part J. Int. Soc. Anal. Cytol.* **2016**, *89*, 325.
- 489 [28] E. Choi-Rhee, H. Schulman, J. E. Cronan, *Protein Sci. Publ. Protein Soc.* **2004**, *13*,
490 3043.
- 491 [29] J. E. Cronan, *J. Nutr. Biochem.* **2005**, *16*, 416.
- 492 [30] A. Chapman-Smith, J. E. Cronan, *Trends Biochem. Sci.* **1999**, *24*, 359.
- 493 [31] S. J. Li, J. E. Cronan, *J. Biol. Chem.* **1992**, *267*, 855.
- 494 [32] K. Kwon, D. Beckett, *Protein Sci. Publ. Protein Soc.* **2000**, *9*, 1530.
- 495 [33] D. I. Kim, K. C. Birendra, W. Zhu, K. Motamedchaboki, V. Doye, K. J. Roux, *Proc.*
496 *Natl. Acad. Sci. U. S. A.* **2014**, *111*, E2453.
- 497 [34] K. J. Roux, D. I. Kim, M. Raida, B. Burke, *J. Cell Biol.* **2012**, *196*, 801.
- 498 [35] D. G. May, K. J. Roux, *Methods Mol. Biol. Clifton NJ* **2019**, *2008*, 83.
- 499 [36] K. J. Roux, D. I. Kim, B. Burke, D. G. May, *Curr. Protoc. Protein Sci.* **2018**, *91*,
500 19.23.1.
- 501 [37] L. T. Oostdyk, L. Shank, K. Jividen, N. Dworak, N. E. Sherman, B. M. Paschal,
502 *Methods San Diego Calif* **2018**, DOI 10.1016/j.ymeth.2018.11.003.
- 503 [38] D. I. Kim, S. C. Jensen, K. A. Noble, B. Kc, K. H. Roux, K. Motamedchaboki, K. J.
504 Roux, *Mol. Biol. Cell* **2016**, *27*, 1188.
- 505 [39] S. De Munter, J. Görnemann, R. Derua, B. Lesage, J. Qian, E. Heroes, E. Waelkens,
506 A. Van Eynde, M. Beullens, M. Bollen, *FEBS Lett.* **2017**, *591*, 415.
- 507 [40] T. C. Branon, J. A. Bosch, A. D. Sanchez, N. D. Udeshi, T. Svinkina, S. A. Carr, J. L.
508 Feldman, N. Perrimon, A. Y. Ting, *Nat. Biotechnol.* **2018**, *36*, 880.
- 509 [41] W. Xie, A. Chojnowski, T. Boudier, J. S. Y. Lim, S. Ahmed, Z. Ser, C. Stewart, B.
510 Burke, *Curr. Biol. CB* **2016**, *26*, 2651.
- 511 [42] C. James, M. Müller, M. W. Goldberg, C. Lenz, H. Urlaub, R. H. Kehlenbach, *J. Biol.*
512 *Chem.* **2019**, DOI 10.1074/jbc.RA118.007283.
- 513 [43] J.-M. Dong, F. P.-L. Tay, H. L.-F. Swa, J. Gunaratne, T. Leung, B. Burke, E. Manser,
514 *Sci. Signal.* **2016**, *9*, rs4.

- 515 [44] G. D. Gupta, É. Coyaud, J. Gonçalves, B. A. Mojarad, Y. Liu, Q. Wu, L.
516 Gheiratmand, D. Comartin, J. M. Tkach, S. W. T. Cheung, M. Bashkurov, M. Hasegan, J. D.
517 Knight, Z.-Y. Lin, M. Schueler, F. Hildebrandt, J. Moffat, A.-C. Gingras, B. Raught, L.
518 Pelletier, *Cell* **2015**, *163*, 1484.
- 519 [45] A. Cole, Z. Wang, E. Coyaud, V. Voisin, M. Gronda, Y. Jitkova, R. Mattson, R.
520 Hurren, S. Babovic, N. Maclean, I. Restall, X. Wang, D. V. Jeyaraju, M. A. Sukhai, S.
521 Prabha, S. Bashir, A. Ramakrishnan, E. Leung, Y. H. Qia, N. Zhang, K. R. Combes, T.
522 Ketela, F. Lin, W. A. Houry, A. Aman, R. Al-Awar, W. Zheng, E. Wienholds, C. J. Xu, J.
523 Dick, J. C. Y. Wang, J. Moffat, M. D. Minden, C. J. Eaves, G. D. Bader, Z. Hao, S. M.
524 Kornblau, B. Raught, A. D. Schimmer, *Cancer Cell* **2015**, *27*, 864.
- 525 [46] S. Konovalova, X. Liu, P. Manjunath, S. Baral, N. Neupane, T. Hilander, Y. Yang, D.
526 Balboa, M. Terzioglu, L. Euro, M. Varjosalo, H. Tyynismaa, *Redox Biol.* **2018**, *19*, 37.
- 527 [47] C. A. Lamb, S. Nühlen, D. Judith, D. Frith, A. P. Snijders, C. Behrends, S. A. Tooze,
528 *EMBO J.* **2016**, *35*, 281.
- 529 [48] A. Caballe, D. M. Wenzel, M. Agromayor, S. L. Alam, J. J. Skalicky, M. Kloc, J. G.
530 Carlton, L. Labrador, W. I. Sundquist, J. Martin-Serrano, *eLife* **2015**, *4*, e06547.
- 531 [49] K. Jacquet, S. L. Banerjee, F. J. M. Chartier, S. Elowe, N. Bisson, *Mol. Cell.*
532 *Proteomics MCP* **2018**, *17*, 1979.
- 533 [50] C. Yeh, É. Coyaud, M. Bashkurov, P. van der Lelij, S. W. T. Cheung, J. M. Peters, B.
534 Raught, L. Pelletier, *Curr. Biol. CB* **2015**, *25*, 2290.
- 535 [51] P. V'kovski, M. Gerber, J. Kelly, S. Pfaender, N. Ebert, S. Braga Lagache, C.
536 Simillion, J. Portmann, H. Stalder, V. Gaschen, R. Bruggmann, M. H. Stoffel, M. Heller, R.
537 Dijkman, V. Thiel, *eLife* **2019**, *8*, DOI 10.7554/eLife.42037.
- 538 [52] M. Ramanathan, K. Majzoub, D. S. Rao, P. H. Neela, B. J. Zarnegar, S. Mondal, J. G.
539 Roth, H. Gai, J. R. Kovalski, Z. Siprashvili, T. D. Palmer, J. E. Carette, P. A. Khavari, *Nat.*
540 *Methods* **2018**, *15*, 207.
- 541 [53] R. J. Austin, T. Xia, J. Ren, T. T. Takahashi, R. W. Roberts, *J. Am. Chem. Soc.* **2002**,
542 *124*, 10966.
- 543 [54] B. Conlan, T. Stoll, J. J. Gorman, I. Saur, J. P. Rathjen, *Front. Plant Sci.* **2018**, *9*,
544 1882.
- 545 [55] A. Mair, S.-L. Xu, T. C. Branon, A. Y. Ting, D. C. Bergmann, *eLife* **2019**, *8*, DOI
546 10.7554/eLife.47864.
- 547 [56] A. Uezu, D. J. Kanak, T. W. A. Bradshaw, E. J. Soderblom, C. M. Catavero, A. C.
548 Burette, R. J. Weinberg, S. H. Soderling, *Science* **2016**, *353*, 1123.
- 549 [57] J. D. Martell, T. J. Deerinck, Y. Sancak, T. L. Poulos, V. K. Mootha, G. E. Sosinsky,
550 M. H. Ellisman, A. Y. Ting, *Nat. Biotechnol.* **2012**, *30*, 1143.
- 551 [58] H.-W. Rhee, P. Zou, N. D. Udeshi, J. D. Martell, V. K. Mootha, S. A. Carr, A. Y.
552 Ting, *Science* **2013**, *339*, 1328.
- 553 [59] N. D. Udeshi, K. Pedram, T. Svinkina, S. Fereshetian, S. A. Myers, O. Aygun, K.

- 554 Krug, K. Clauser, D. Ryan, T. Ast, V. K. Mootha, A. Y. Ting, S. A. Carr, *Nat. Methods* **2017**,
555 DOI 10.1038/nmeth.4465.
- 556 [60] V. Hung, N. D. Udeshi, S. S. Lam, K. H. Loh, K. J. Cox, K. Pedram, S. A. Carr, A. Y.
557 Ting, *Nat. Protoc.* **2016**, *11*, 456.
- 558 [61] S. S. Lam, J. D. Martell, K. J. Kamer, T. J. Deerinck, M. H. Ellisman, V. K. Mootha,
559 A. Y. Ting, *Nat. Methods* **2014**, *12*, 51.
- 560 [62] Y. Han, T. C. Branon, J. D. Martell, D. Boassa, D. Shechner, M. H. Ellisman, A. Ting,
561 *ACS Chem. Biol.* **2019**, DOI 10.1021/acscchembio.8b00919.
- 562 [63] X. D. Gao, L.-C. Tu, A. Mir, T. Rodriguez, Y. Ding, J. Leszyk, J. Dekker, S. A.
563 Shaffer, L. J. Zhu, S. A. Wolfe, E. J. Sontheimer, *Nat. Methods* **2018**, DOI 10.1038/s41592-
564 018-0006-2.
- 565 [64] S. A. Myers, J. Wright, R. Peckner, B. T. Kalish, F. Zhang, S. A. Carr, *Nat. Methods*
566 **2018**, *15*, 437.
- 567 [65] C.-L. Chen, Y. Hu, N. D. Udeshi, T. Y. Lau, F. Wirtz-Peitz, L. He, A. Y. Ting, S. A.
568 Carr, N. Perrimon, *Proc. Natl. Acad. Sci. U. S. A.* **2015**, *112*, 12093.
- 569 [66] V. Hung, P. Zou, H.-W. Rhee, N. D. Udeshi, V. Cracan, T. Svinkina, S. A. Carr, V. K.
570 Mootha, A. Y. Ting, *Mol. Cell* **2014**, *55*, 332.
- 571 [67] S.-Y. Lee, M.-G. Kang, J.-S. Park, G. Lee, A. Y. Ting, H.-W. Rhee, *Cell Rep.* **2016**,
572 *15*, 1837.
- 573 [68] D. U. Mick, R. B. Rodrigues, R. D. Leib, C. M. Adams, A. S. Chien, S. P. Gygi, M. V.
574 Nachury, *Dev. Cell* **2015**, *35*, 497.
- 575 [69] J. Hwang, P. J. Espenshade, *Biochem. J.* **2016**, *473*, 2463.
- 576 [70] S. Han, N. D. Udeshi, T. J. Deerinck, T. Svinkina, M. H. Ellisman, S. A. Carr, A. Y.
577 Ting, *Cell Chem. Biol.* **2017**, *24*, 404.
- 578 [71] B. T. Lobingier, R. Hüttenhain, K. Eichel, K. B. Miller, A. Y. Ting, M. von Zastrow,
579 N. J. Krogan, *Cell* **2017**, *169*, 350.
- 580 [72] J. Paek, M. Kalocsay, D. P. Staus, L. Wingler, R. Pascolutti, J. A. Paulo, S. P. Gygi,
581 A. C. Kruse, *Cell* **2017**, *169*, 338.
- 582 [73] P. Kaewsapsak, D. M. Shechner, W. Mallard, J. L. Rinn, A. Y. Ting, *eLife* **2017**, *6*,
583 DOI 10.7554/eLife.29224.
- 584 [74] F. M. Fazal, S. Han, K. R. Parker, P. Kaewsapsak, J. Xu, A. N. Boettiger, H. Y.
585 Chang, A. Y. Ting, *Cell* **2019**, DOI 10.1016/j.cell.2019.05.027.
- 586 [75] A. Padrón, S. Iwasaki, N. T. Ingolia, *Mol. Cell* **2019**, *75*, 875.
- 587 [76] Y. Zhou, G. Wang, P. Wang, Z. Li, T. Yue, J. Wang, P. Zou, *Angew. Chem. Int. Ed*
588 *Engl.* **2019**, DOI 10.1002/anie.201905949.
- 589 [77] M. S. Dickinson, L. N. Anderson, B.-J. M. Webb-Robertson, J. R. Hansen, R. D.
590 Smith, A. T. Wright, K. Hybiske, *PLoS Pathog.* **2019**, *15*, e1007698.

- 591 [78] E. A. Rucks, M. G. Olson, L. M. Jorgenson, R. R. Srinivasan, S. P. Ouellette, *Front.*
592 *Cell. Infect. Microbiol.* **2017**, 7, 40.
- 593 [79] M. G. Olson, L. M. Jorgenson, R. E. Widner, E. A. Rucks, *Methods Mol. Biol. Clifton*
594 *NJ* **2019**, 2042, 245.
- 595 [80] M. G. Olson, R. E. Widner, L. M. Jorgenson, A. Lawrence, D. Lagundzin, N. T.
596 Woods, S. P. Ouellette, E. A. Rucks, *Infect. Immun.* **2019**, IAI.00537.
- 597 [81] U. S. Ganapathy, L. Bai, L. Wei, K. A. Eckartt, C. M. Lett, M. L. Previti, I. S. Carrico,
598 J. C. Seeliger, *ACS Infect. Dis.* **2018**, 4, 918.
- 599 [82] Á. Ástvaldsson, K. Hultenby, S. G. Svärd, J. Jerlström-Hultqvist, *mSphere* **2019**, 4,
600 DOI 10.1128/mSphereDirect.00153-19.
- 601 [83] Y. G. Santin, T. Doan, R. Lebrun, L. Espinosa, L. Journet, E. Cascales, *Nat.*
602 *Microbiol.* **2018**, 3, 1304.
- 603 [84] Y. Akhter, S. Thakur, *Microbiol. Res.* **2017**, 204, 9.
- 604 [85] M. J. Pearce, J. Mintseris, J. Ferreyra, S. P. Gygi, K. H. Darwin, *Science* **2008**, 322,
605 1104.
- 606 [86] F. Striebel, F. Imkamp, D. Özcelik, E. Weber-Ban, *Biochim. Biophys. Acta* **2014**,
607 1843, 103.
- 608 [87] J. Barandun, C. L. Delley, E. Weber-Ban, *BMC Biol.* **2012**, 10, 95.
- 609 [88] M. I. Samanovic, K. H. Darwin, *Trends Microbiol.* **2016**, 24, 26.
- 610 [89] E. Guth, M. Thommen, E. Weber-Ban, *J. Biol. Chem.* **2011**, 286, 4412.
- 611 [90] F. Striebel, F. Imkamp, M. Sutter, M. Steiner, A. Mamedov, E. Weber-Ban, *Nat.*
612 *Struct. Mol. Biol.* **2009**, 16, 647.
- 613 [91] T. Wang, K. H. Darwin, H. Li, *Nat. Struct. Mol. Biol.* **2010**, 17, 1352.
- 614 [92] Q. Liu, J. Zheng, W. Sun, Y. Huo, L. Zhang, P. Hao, H. Wang, M. Zhuang, *Nat.*
615 *Methods* **2018**, 15, 715.
- 616 [93] S. Urlinger, U. Baron, M. Thellmann, M. T. Hasan, H. Bujard, W. Hillen, *Proc. Natl.*
617 *Acad. Sci. U. S. A.* **2000**, 97, 7963.
- 618 [94] L. A. Banaszynski, C. W. Liu, T. J. Wandless, *J. Am. Chem. Soc.* **2005**, 127, 4715.
- 619 [95] D. I. Kim, J. A. Cutler, C. H. Na, S. Reckel, S. Renuse, A. K. Madugundu, R. Tahir,
620 H. L. Goldschmidt, K. L. Reddy, R. L. Haganir, X. Wu, N. E. Zachara, O. Hantschel, A.
621 Pandey, *J. Proteome Res.* **2017**, DOI 10.1021/acs.jproteome.7b00775.
- 622 [96] J. A. Groves, A. O. Maduka, R. N. O'Meally, R. N. Cole, N. E. Zachara, *J. Biol.*
623 *Chem.* **2017**, 292, 6493.
- 624 [97] N. Opitz, K. Schmitt, V. Hofer-Pretz, B. Neumann, H. Krebber, G. H. Braus, O.
625 Valerius, *Mol. Cell. Proteomics MCP* **2017**, 16, 2199.
- 626 [98] J. A. Ankney, A. Muneer, X. Chen, *Annu. Rev. Anal. Chem. Palo Alto Calif* **2018**, 11,

- 627 49.
- 628 [99] A. Azhar, G. W. Booker, S. W. Polyak, *Biochem. Anal. Biochem.* **2015**, *4*, 210.
- 629 [100] M. Larochele, D. Bergeron, B. Arcand, F. Bachand, *J. Cell Sci.* **2019**, *132*, DOI
630 10.1242/jcs.232249.
- 631 [101] Y. Zhang, G. Song, N. K. Lal, U. Nagalakshmi, Y. Li, W. Zheng, P.-J. Huang, T. C.
632 Branon, A. Y. Ting, J. W. Walley, S. P. Dinesh-Kumar, *Nat. Commun.* **2019**, *10*, 3252.
- 633 [102] K. H. Loh, P. S. Stawski, A. S. Draycott, N. D. Udeshi, E. K. Lehrman, D. K. Wilton,
634 T. Svinkina, T. J. Deerinck, M. H. Ellisman, B. Stevens, S. A. Carr, A. Y. Ting, *Cell* **2016**,
635 *166*, 1295.
- 636 [103] N. Kotani, J. Gu, T. Isaji, K. Udaka, N. Taniguchi, K. Honke, *Proc. Natl. Acad. Sci. U.*
637 *S. A.* **2008**, *105*, 7405.
- 638 [104] K. Honke, A. Miyagawa-Yamaguchi, N. Kotani, *Methods Mol. Biol. Clifton NJ* **2019**,
639 *2008*, 1.
- 640 [105] J. S. Rees, *Methods Mol. Biol. Clifton NJ* **2019**, *2008*, 13.
- 641 [106] J. S. Rees, X.-W. Li, S. Perrett, K. S. Lilley, A. P. Jackson, *Curr. Protoc. Protein Sci.*
642 **2015**, *80*, 19.27.1.
- 643 [107] X.-W. Li, J. S. Rees, P. Xue, H. Zhang, S. W. Hamaia, B. Sanderson, P. E. Funk, R.
644 W. Farndale, K. S. Lilley, S. Perrett, A. P. Jackson, *J. Biol. Chem.* **2014**, *289*, 14434.
- 645 [108] D. B. Beck, R. Bonasio, *Curr. Protoc. Chem. Biol.* **2017**, *9*, 128.
- 646 [109] Z. B. Hill, S. B. Pollock, M. Zhuang, J. A. Wells, *J. Am. Chem. Soc.* **2016**, *138*, 13123.
- 647 [110] M. Zhuang, S. Guan, H. Wang, A. L. Burlingame, J. A. Wells, *Mol. Cell* **2013**, *49*,
648 273.
- 649 [111] B. van Steensel, S. Henikoff, *Nat. Biotechnol.* **2000**, *18*, 424.
- 650 [112] F. Cléard, F. Karch, R. K. Maeda, *Methods Mol. Biol. Clifton NJ* **2014**, *1196*, 279.
- 651 [113] V. Visone, W. Han, G. Perugino, G. Del Monaco, Q. She, M. Rossi, A. Valenti, M.
652 Ciaramella, *PloS One* **2017**, *12*, e0185791.
- 653 [114] P. V. Escribá, X. Busquets, J. Inokuchi, G. Balogh, Z. Török, I. Horváth, J. L.
654 Harwood, L. Vigh, *Prog. Lipid Res.* **2015**, *59*, 38.

655

656 **Legend to Figures**

657 **Figure 1.** Schematic representation of conventional methods used for detection of PPIs. **a)** Co-
658 immunoprecipitation workflow. From left to right: cellular proteins are extracted from cells and
659 incubated with specific antibody-coated beads directed against a protein of interest (green). The

660 protein of interest and its direct (blue) and indirect (yellow) partners are then co-
661 immunoprecipitated. Detection of PPIs is achieved by Western Blot analysis (Total, total
662 proteins in cellular extract; Co-IP, partners co-immunoprecipitated with the protein of interest)
663 **b) Two-hybrid assay.** Two-hybrid assay is based on the reconstitution of a specific protein
664 (adenylate cyclase for BACTH and Gal4 for Y2H) that consists in two domains (light and dark
665 grey). Bait (in green) and prey (in blue or red) proteins are translationally fused to isolated
666 domains. Spatial association between bait and prey proteins restores the proximity of the two
667 domains and then the protein activity, leading *in fine* to the transcription of a reporter gene. **c)**
668 FRET assay. A bait (in green) and a prey (in blue or red) protein are translationally fused in
669 tandem to fluorescent proteins. An example is showed with the cyan fluorescent protein (CFP,
670 cyan) and the yellow fluorescent protein (YFP, yellow). Energy transfer (i.e., FRET) between
671 fluorescent reporters can occur if the bait and the prey proteins are within 10 nm of distance
672 (left panel). The loss of fluorescence intensity from the donor (CFP) and the increase of
673 fluorescence intensity from the acceptor (YFP) can be visualized by monitoring fluorescence
674 spectra (right panel).

675

676 **Figure 2.** BioID workflow. Fusion between BioID protein (blue) and a bait protein (black) is
677 expressed in native context within cells. *In vivo* labeling (blue radius) is initiated by the addition
678 of a supra-physiological concentration of biotin during many hours. Cells are then lysed, and
679 biotinylated proteins are purified by enrichment on streptavidin beads. Trypsin digestion
680 provides the generation of peptides that are then identified by mass spectrometry.

681

682 **Figure 3.** APEX proximity-dependent biotin labeling workflow. Fusion between APEX2
683 protein (blue) and a bait protein (black) is expressed in native context within cells. After
684 incubation in presence of biotin-phenol, a H₂O₂ pulse allows biotin labeling (red radius) of both

685 direct partners (yellow and green) and proteins in close environment of the bait protein (brown).
686 While unbiotinylated proteins are washed, biotinylated proteins are purified by enrichment on
687 streptavidin beads after cell lysis. Trypsin digestion provides the generation of peptides that are
688 then identified by mass spectrometry.

689

690 **Figure 4.** PUP-IT workflow for intra and extracellular labeling. **a)** For intracellular labeling,
691 the cytosolic domain of the membrane receptor CD28 (blue) is fused to the PUP ligase PafA
692 (green). The expression of the bio-Pup(E) substrate is under the control of TET-ON system.
693 Addition of doxycycline (Dox) induces bio-Pup(E) production and initiates the PafA-mediated
694 labeling (green radius). **b)** For cell surface labeling, the extracellular domain of the membrane
695 receptor CD28 (blue) and PafA (green) are fused to specific adaptors, FKBP and FRB,
696 respectively. Addition of rapamycin (purple pill) allows the link between the two adaptors and
697 hence, the formation of a functional PUP-IT complex. PafA-mediated labeling (green radius)
698 is initiated upon the addition of ATP and truncated bio-Pup(E) peptides (bio-DE28).

699

700 **Figure 5.** Schematic pipelines for major quantitative approaches used for proximity-tagging
701 quantification. For each approach, 1 corresponds to the negative control (without tagging
702 enzyme), 2 corresponds to the specificity control (where the tagging enzyme is independently
703 expressed in the same cellular compartment that the bait protein), and 3 corresponds to the test
704 (the bait protein is fused to the tagging enzyme). **a)** Three-state SILAC experiment. Cells are
705 grown in presence of light (L, yellow, negative control), medium (M, blue, specificity control)
706 or heavy (H, red, test) stable isotope–enriched amino acids. Upon proximity labeling, L, M and
707 H protein extracts are combined at equal ratio before further processing. Biotinylated proteins
708 are then enriched, digested and quantified by LC-MS/MS analysis. In this case, H/L intensity
709 ratio represents the extent of biotinylation by the tagging enzyme and H/M intensity ratio

710 represents the extent of specific biotinylation by the tagging enzyme versus non-specific
711 endogenous proteins. **b)** Triplex TMT experiment. Cells are grown in standard conditions.
712 Upon proximity labeling, biotinylated proteins are enriched, digested and then chemically
713 tagged with MS-differentiable TMT labels (126, red, negative control; 127, blue, specificity
714 control; 128, green, test). Tagged-peptides are combined at equal ratio and quantified by LC-
715 MS/MS analysis. 128/126 intensity ratio is used to distinguish the extent of biotinylation by the
716 tagging enzyme and 128/127 intensity ratio represents the extent of specific biotinylation by
717 the tagging enzyme versus non-specific endogenous proteins. **c)** LFQ assay. Cells are grown in
718 standard conditions. Upon proximity labeling, biotinylated proteins are enriched and digested.
719 Samples are then independently quantified and compared by using ion intensity or spectral
720 counting (as represented).
721

Figure 1.

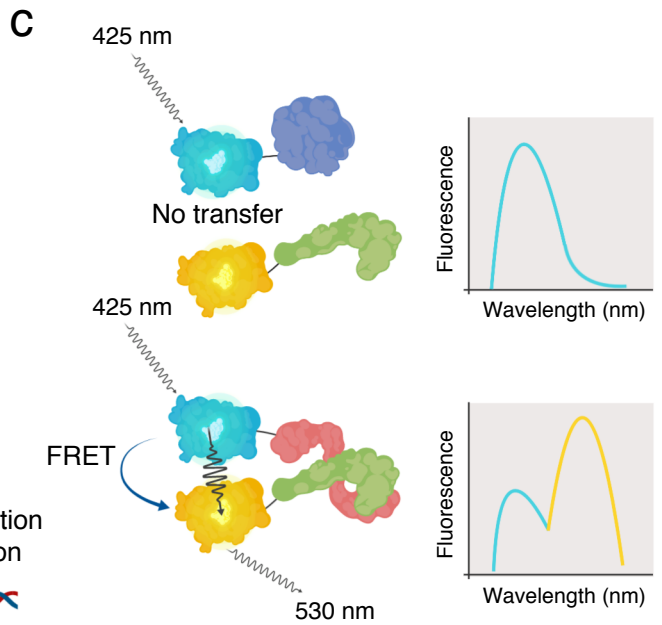
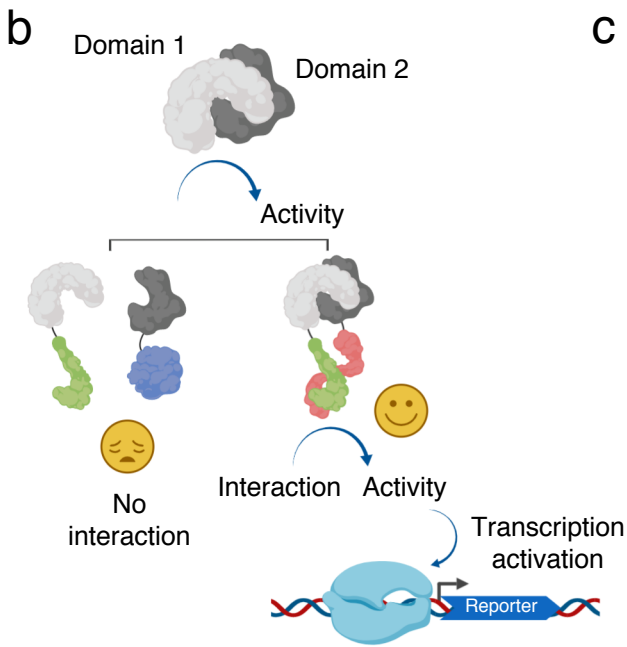
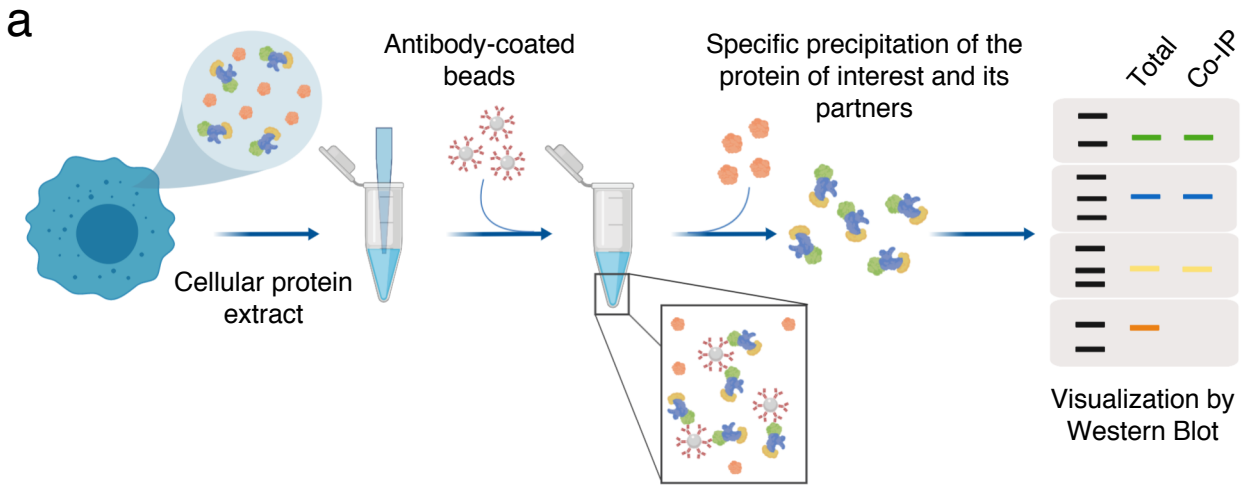


Figure 2.

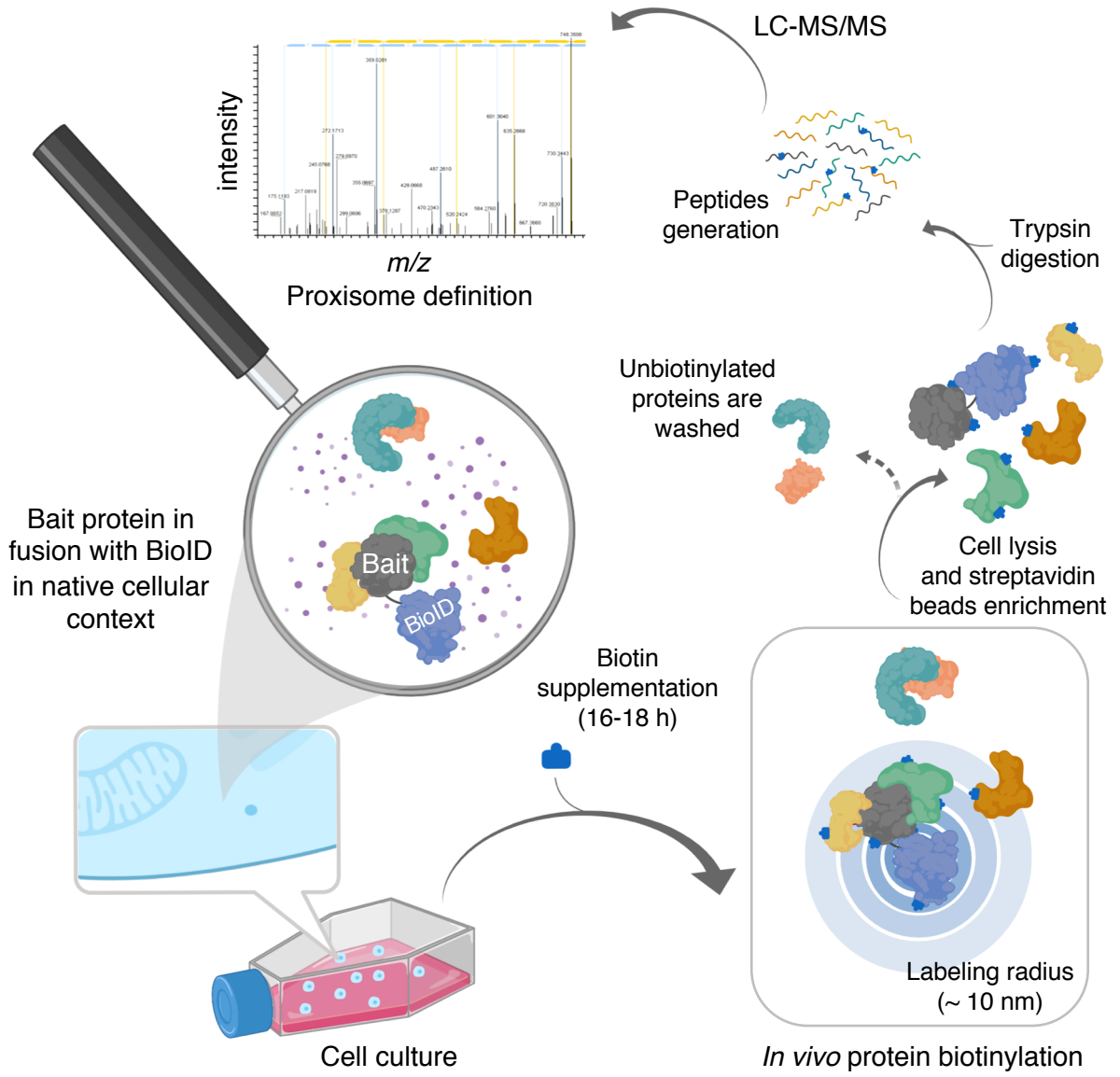


Figure 3.

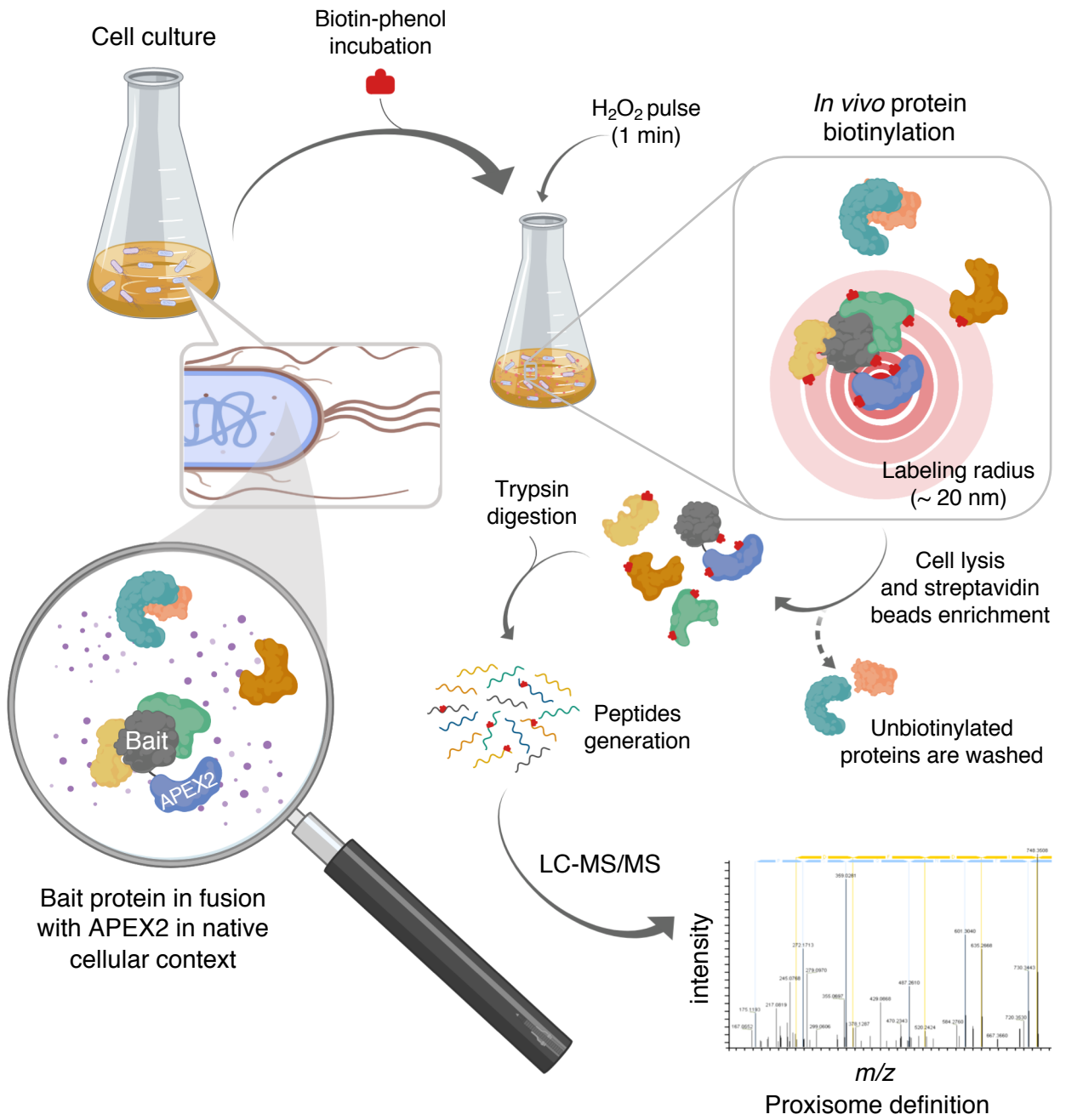


Figure 4.

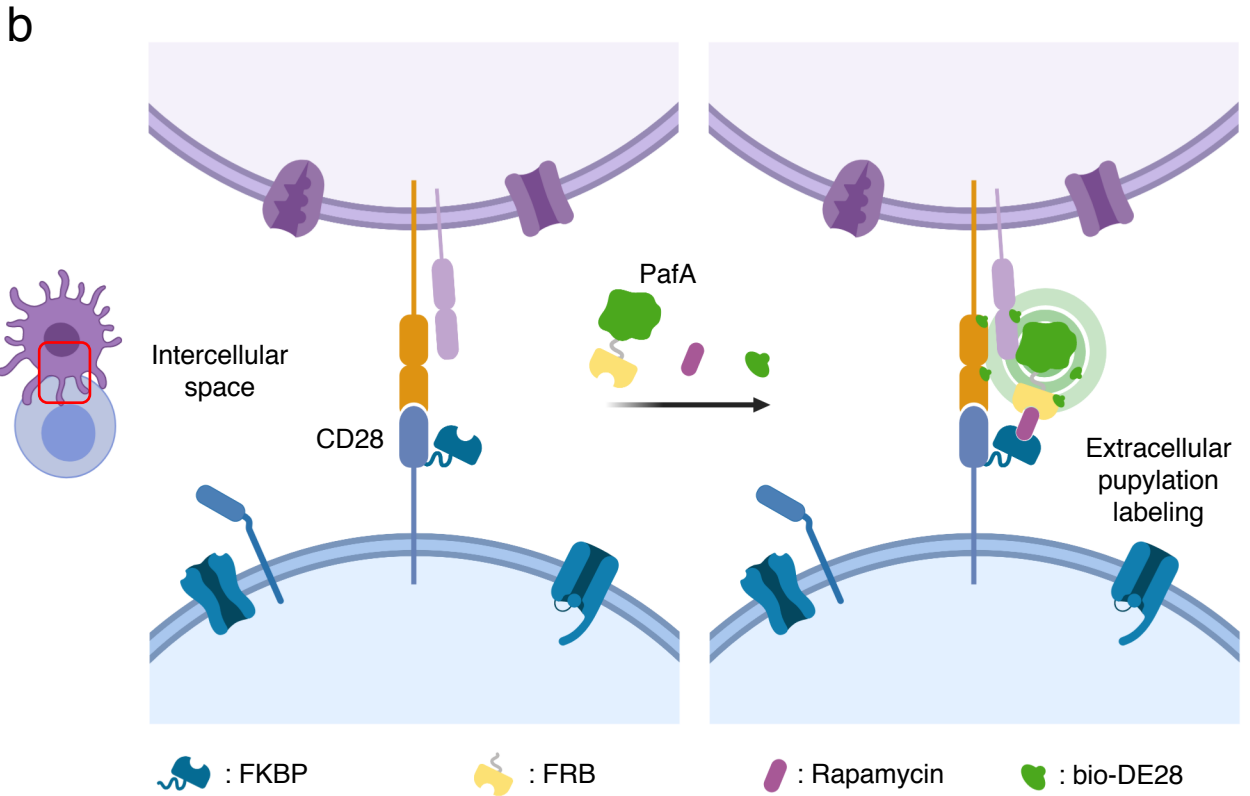
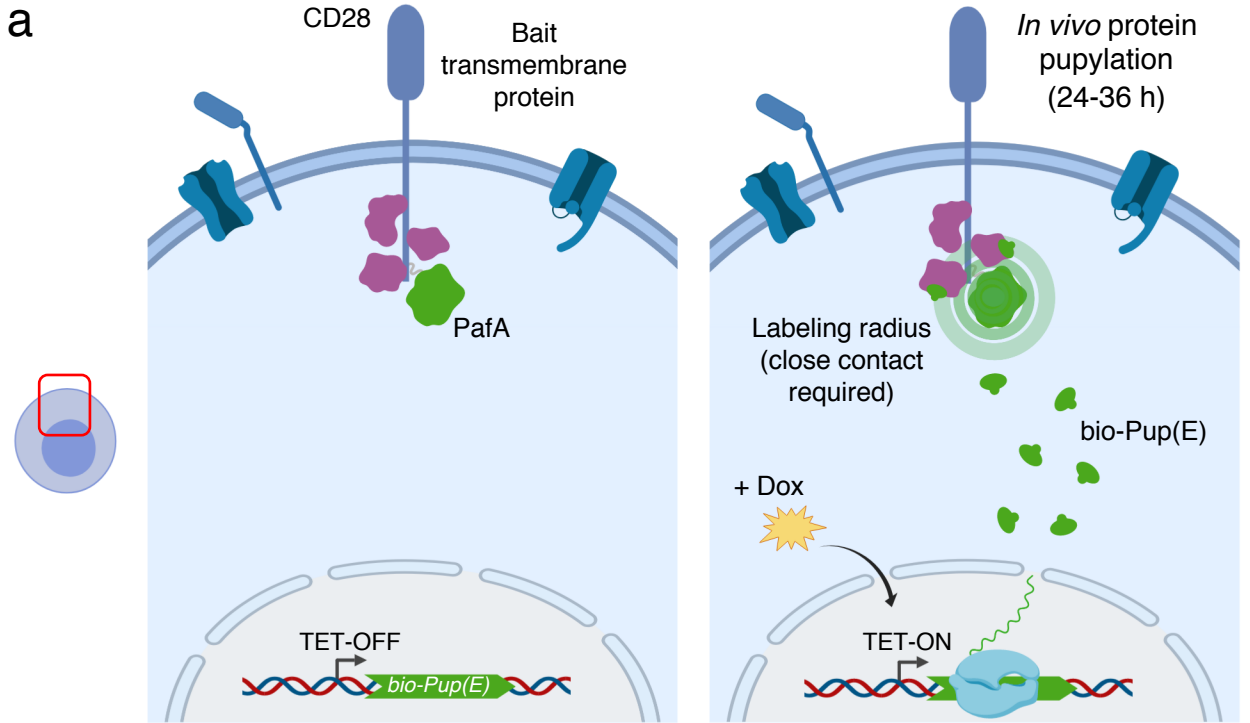


Figure 5.

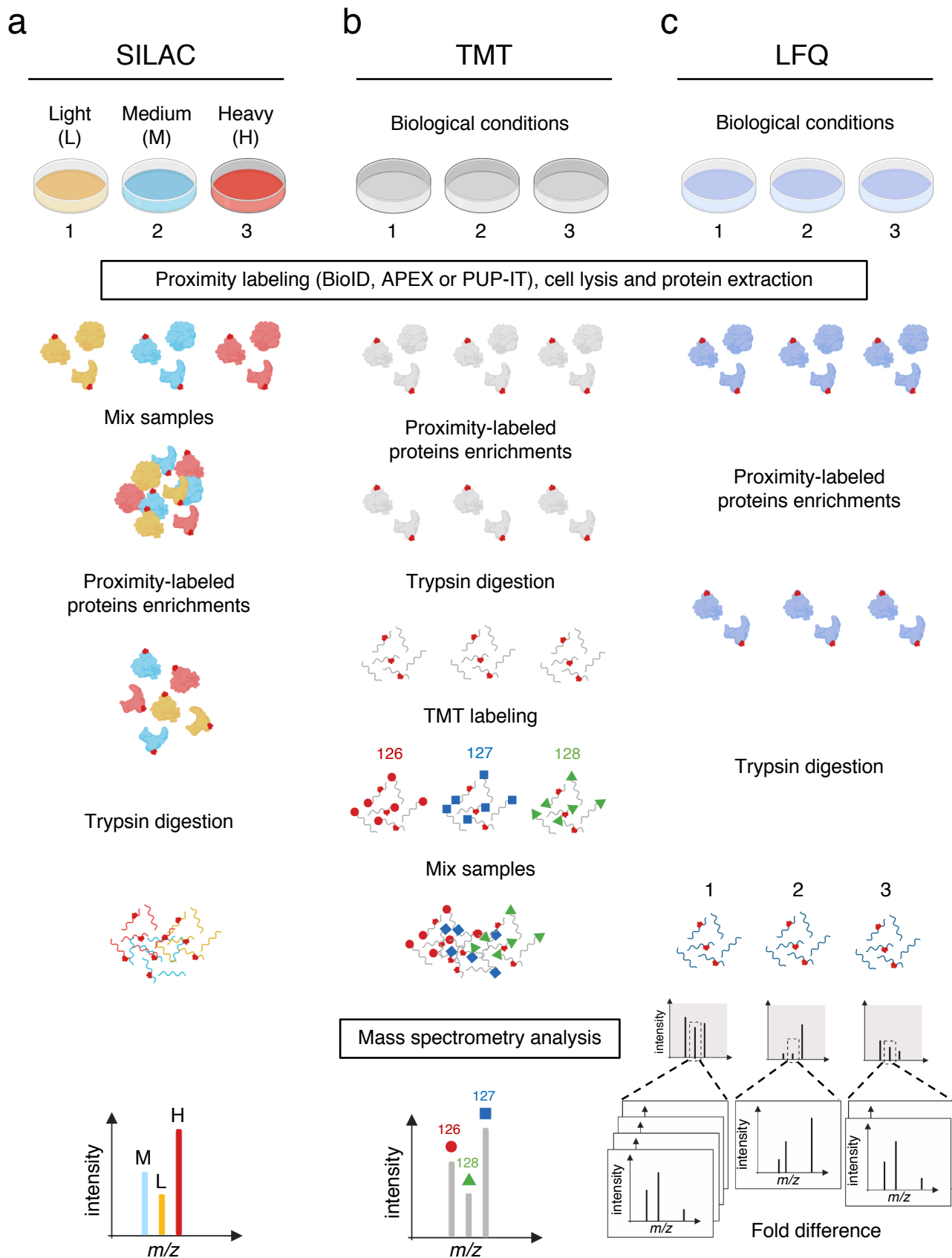


Table 1. Comparative table of the main features of the different proximity-tagging methods

	BioID	(mini)TurboID	APEX	PUP-IT
Origin	Bacteria (BirA from <i>Escherichia coli</i>)	Bacteria (BirA from <i>Escherichia coli</i>)	Plantae (APX from <i>Glycine max</i>)	Bacteria (PafA from <i>Corynebacterium glutamicum</i>)
Molecular mass	35 kDa (for BioID) 27 kDa (for BioID2)	28 kDa (for miniTurbo) 35 kDa (for TurboID)	27 kDa	54 kDa
Substrates	Biotin and ATP	Biotin and ATP	H ₂ O ₂ and phenol derivative-molecules	Pup(E) derivative-peptides and ATP
Range of temperature ^a	37°C for BioID and 37°C to 50°C for BioID2	20°C to 37°C	30°C to 37°C	37°C
Enzyme activity ^b (at 37°C)	+	+++	++++	++
Time of labeling	16-18 hours	10 min to several hours (depending on the organism)	1 min	24-36 hours
Labeling radius	10-15 nm	10-15 nm	20 nm	Very close contact
Labeled macromolecules	Proteins	Proteins	Proteins and nucleic acids	Proteins
Labeled residues	Lys	Lys	Tyr (98%) and Trp, His, Cys (2%) for proteins; mostly guanosine for nucleic acids	Lys
Temporal control (labeling initiation)	No	No	Yes	No
Information about the POI	Long history	Intermediate	Snapshot	Long history

^a Enzyme works at these temperatures but temperatures between this range have not necessary been tested

^b +++++, strong activity; +++, very good activity; ++, good activity; +, weak activity